International Meeting on Reduced Enrichment for Research and Test Reactors (RERTR), Petten, The Netherlands, 14-16 October 1985

INIS-XA-C--064

DEVELOPMENT OF HEAT TRANSFER PACKAGE FOR CORE THERMAL-HYDRAULIC DESIGN AND ANALYSIS OF UPGRADED JRR-3

Yukio SUDO, Hiromasa IKAWA and Masanori KAMINAGA

Japan Atomic Energy Research Institute (JAERI)

Tokai-mura, Ibaraki-ken, Japan 319-11

Abstract

A heat transfer package was developed for the core thermal-hydraulic design and analysis of the Japan Research Reactor-3 (JRR-3) which is to be remodeled to a 20 MWt pool-type, light water-cooled reactor with 20 % low enriched uranium (LEU) plate-type fuel. This paper presents the constitution of the developed heat transfer package and the applicability of the heat transfer correlations adopted in it, based on the heat transfer experiments in which thermal-hydraulic features of the new JRR-3 core were properly reflected.

I INTRODUCTION

At the Japan Atomic Energy Research Institute, the Japan Research Reactor-3 (JRR-3) is now under remodelling into a 20 MWt light water moderated and cooled, beryllium and heavy water reflected, pool-type reactor with 20 % low enriched uranium plate-type fuel. For a reference, Figure 1 shows a schematic diagram of the reactor including a core, a light water primary cooling system and a heavy water cooling system. The major features of the JRR-3 for the thermal-hydraulic design and safety analysis are as follows. (1) Two modes are adopted for core cooling under normal operation, one is a natural-convection cooling with upflow in the core for low core power up to 200 KW and the other is a forced-convection cooling for high core power up to 20 MW. Flow direction in the core for the forced-convection cooling mode is downward from the

viewpoint of attenuation of ^{16}N. With downflow in the core at the normal operation, a core flow reversal should occur to remove the decay heat after scram with upflow in some of operational transients and accidents assumed in the safety design. (2) Two major design criteria have been set up for the core thermal-hydraulics so that fuel plates may have enough safety margin for the condition of normal operation. One is to avoid nucleate boiling of coolant anywhere in the core and the other is to keep the minimum DNBR not less than 1.5.

This paper introduces the heat transfer experiments in which key thermal-hydraulic features of the new JRR-3 core were properly reflected and presents the constitution of the heat transfer package for the core thermal-hydraulic design and safety analysis.

II HEAT TRANSFER EXPERIMENTS FOR DEVELOPMENT OF HEAT TRANSFER PACKAGE

1. Experimental Rig Figure 2 shows a schematic diagram of the test loop which is used to develope the heat transfer package for the new JRR-3. Either upflow or downflow can be selected in the test.

The test section is composed of a flow channel, a lower plenum and an upper plenum. The configuration of the flow channel which is composed of two adjacent heating plates is rectangular with 50 mm in width, 2.25 mm in water gap and 750 mm in length. The heating plates are made of Inconel 600 with 1.0 mm in thickness.

2. ONB Conditions The ONB temperature has been determined by the following two simultaneous equations in the thermal-hydraulic design under normal operation with forced-convection.

$$q = 1.76 \times 10^{-3} \cdot P^{1.156}\left\{\frac{9}{5}(T_W - T_s)\right\}, \frac{2.83}{P^{0.0234}} \quad (1)$$

$$q = 0.023 R_e^{0.8} P_r^{0.4} \frac{k}{D_e}\left\{(T_W - T_s) + (T_s - T_b)\right\}. \quad (2)$$

Equation (1) was proposed by Bergles and Rohsenow[1] for water, and Eq. (2) was proposed by Dittus and Boelter[2] for the forced con- tion single-phase flow. For the evaluation of the margin of fuel surface temperature against the ONB temperature, the precision of Eqs. (1) and (2) should have been made clear. The precision of Eq. (1) was not always clear for the application to the subchannel of the JRR-3 because the amount of the available data was small for the forced convection downflow though some data for upflow have been reported.[3,5]

Figure 3 shows the comparison of the experimental results obtained for both upflow and downflow in this experiment with Eq. (1), with respect to the relationship of q vs ΔT_s at the onset of nucleate boiling. It can be pointed out in this figure that no significant difference between upflow and downflow is observed with

respect to the relationship of q vs ΔT_s at the onset of nucleate boiling.

Figure 4 shows the comparison of the experimental results including the available existing data[1,3,4,5] with the predictions by Eq. (1) in order to evaluate the error of Eq. (1). This figure clearly indicates that the error of Eq. (1) is about -1 K against the lower limit of the measured superheats at the onset of nucleate boiling.

3. Forced-Convection Single-Phase Flow The problem is the differences in the single-phase forced-convection heat transfer characteristics between upflow and downflow for a vertical retangular channel simulating a JRR-3 subchannel. It is considered that there are no differences in the single-phase forced-convection heat transfer characteristics between upflow and downflow for a high velocity at the normal operation condition of the JRR-3. The effects of buoyant force should, however, enhance the heat transfer for upflow and on the contrary, decrease the heat transfer for downflow at low velocities, which should occur during the operational transients and accidents.

Figure 5 shows the comparison of the experimental results for Re larger than 1,000 with the existing correlations proposed by Dittus-Boelter[2], Sieder-Tate[6] and Colburn[7] for turbulent forced-convection heat transfer.

The characteristics of the turbulent forced-convection heat transfer for narrow vertical flow channel are summarized for both upflow and downflow as follows. (1) By use of equivalent hydraulic diameter for rectangular channel, any existing heat transfer correlation of Dittus-Boelter, Sieder-Tate and Colburn is available for both upflow and downflow even in the channel whose gap is as narrow as 2.25 mm. (2) No significant differences were observed between upflow and downflow in turbulent forced-convection heat transfer characteristics and therefore, it is considered that there are no effects of buoyant force for the turbulent flow.

For Re less than 2,000 at which the flow is laminar, Fig. 6 shows the comparison of experimental results on Nu for upflow with those for downflow. It is obviously recognized that Nu at downflow are smaller than those at upflow for Re less than about 700. Upper limits of Nu correspond to Nu at the inlet of channel (x = 0 m) and lower limits to Nu at the end of heating plates (x = 0.75 m). For almost the same Re, Nu decrease with the increase of distance x from the inlet of channel for both upflow and downflow.

In order to make clear the effects of buoyant force, Fig. 7 is presented by adopting Grashof number Gr for the abscissa and Nu/Nuo for the ordinate. Here, Nuo is the Nusselt number obtained for the rectangular channel heated from both sides from the analysis by Hwang[8] et al. The effects of buoyant force are evident in the downflow for Re less than about 700 and Gr larger than about 1,000.

4. DNB Heat Flux The major features of DNB heat flux to be predicted for the JRR-3 subchannel are; (i) The flow channel is rectangular with a narrow gap of 2.28 mm and is long with a large

length-to-hydraulic diameter ratio ℓ/De of 170, (ii) the coolant velocity range of interest is fairly wide ranging from downflow to upflow, and (iii) the coolant conditions are at low pressure and low temperature. Among a small amount of experiments with rectangular channel, the study conducted by Mishima[9,10] is most important in the viewpoint of application to the JRR-3 subchannel. But, the errors of the correlations proposed by Mishima and the conditions under which the correlations can be applied have not always been made clear primarily because the quantity of experimental data is very small.

Figure 8 shows all the available DNB heat flux data obtained for upflow both in the rectangular channels and in other channels.[11] The bold line gives a correlation of q^*_{DNB} vs G^* shown below.

$$q^*_{DNB,1} = 0.005\ G^{*\,0.611} \tag{3}$$

Equation (3) corresponds to 1.5 times the lower limit of the data, and is recommended as a DNB heat flux correlation for upflow at not very small G^* not only in the rectangular channels but also in other channels.

Figure 9 shows all the available DNB heat flux data obtained for downflow both in the rectangular channels and in other channels. From this figure it is clear that q^*_{DNB} for downflow both in the rectangular channels and in other channels are lower than those for upflow at low G^* of about 2 ∿ 400. On the other hand, it appears that q^*_{DNB} is almost the same between upflow and downflow at high G^* larger than 400 and at very low G^* including zero.

Figure 10 presents the scheme of DNB heat flux correlations proposed in this study for upflow and downflow. The scheme proposed in this study are composed of three correlations, Eqs. (3), (4) and (5). Eqs. (4) and (5) are expressed as follows.

$$q^*_{DNB,2} = \frac{A}{A_H}\,\frac{\Delta h_i}{h_{fg}}\,G^* \qquad \text{for downflow} \tag{4}$$

$$q^*_{DNB,3} = 0.7(A/A_H)\left[W/\lambda\right]^{1/2}/\left[1+(\gamma_g/\gamma_\ell)^{1/4}\right]^2 \qquad \text{for upflow and downflow} \tag{5}$$

The errors of these correlations were evaluated in the viewpoint of safety design and analysis. Equation (3) is a new correlation for predicting the DNB heat flux for upflow, and Eqs. (4) and (5) are correlations proposed by Mishima.[10] For downflow, there are three regions, Regions I, II and III. In region I, the DNB heat flux is predicted by Eq. (5), which is the same as the correlation predicting the minimum DNB heat flux for upflow. In Region II, the DNB heat flux is predicted by Eq. (4), which gives much lower heat flux than Eq. (3) at the same G^*. In Region III, the DNB heat flux is predicted by Eq. (3), which is the same as the correlation for upflow.

III CONSTITUTION OF HEAT TRANSFER PACKAGE

(1) Single-phase forced-convection flow: For a downward flow, the following were adopted depending on Reynolds number Re.

$$Nu = 4.0 \qquad \text{for laminar flow } (Re < 2000), \quad (6)$$

$$Nu = 0.023\, Re^{0.8} Pr^{0.4} \qquad \text{for turbulent flow } (Re \geq 2500), \quad (7)$$

and Nu is evaluated by interpolation with Eqs. (6) and (7) for transition region ($2000 \leq Re < 2500$).

For an upward flow in a natural-convection cooling mode, the following were provided taking into account the effect of buoyant force.

$$Nu = \max[\text{Eq. (6)}, \text{Collier correlation}] \quad \text{for laminar flow } (Re < 2000), \quad (8)$$

where Collier correlation is given as follows.[12]

$$Nu = 0.17\, Re_f^{0.33} Pr_f^{0.43} \{Pr_f/Pr_w\}^{1/4} \{g\beta D_e^3 (T_w - T_b)/\nu^2\}_f^{0.1} \quad (9)$$

The scheme of heat transfer correlations for single-phase forced-convection flow described above is applied for both liquid flow and steam flow.

(2) ONB Temperature: Eq. (1) is adopted for the correlation predicting the onset of nucleate boiling (ONB) temperature both for upflow and downflow.

(3) Nucleate Boiling Heat Transfer: The following correlation which was developed by Chen[13] are adopted for the heat flux under the subcooled and saturated nucleate boiling.

$$q = 0.023\{R_{e\ell}(1-x)\}^{0.8} \cdot Pr^{0.4} \cdot \frac{k_\ell}{D_E} \cdot (T_W - T_\ell) \cdot F + S \cdot 0.00122 \left[\frac{k_\ell^{0.79} C_{p\ell}^{0.45} \rho_\ell^{0.49}}{\sigma^{0.5} \mu_\ell^{0.29} h_{fg}^{0.24} \rho_g^{0.24}} \right] (T_w - T_s)^{1.24} (P_w - P_s)^{0.75} \quad (10)$$

The factors F and S are determined depending on flow conditions (subcooled boiling or saturated boiling, and so on). It has been confirmed that Eq. (10) can be applied also for downflow, from the comparison with the existing available test data for downflow.[14]

(4) DNB Heat Flux Scheme: A scheme of DNB heat flux correlation for upflow and downflow is composed of Eqs. (3), (4) and (5).

(5) Transition Boiling Heat Transfer and MSFB Temperature: In the heat transfer package, the following correlation which was proposed by Bjonard and Griffith[15] is adopted for the heat flux in the transition boiling region:

$$q = \delta q_{DNB} + (1-\delta) q_{MSFB}, \quad \text{where } \delta = \left(\frac{T_W - T_{MSFB}}{T_{DNB} - T_{MSFB}} \right)^2 . \quad (11)$$

The minimum stable film boiling (MSFB) temperature is defined by the following correlation proposed by Henry[16],

$$T_{MSFB} = T_{HN} + (T_{HN}-T_{\ell})\sqrt{(\gamma k C_p)_{\ell}/(\gamma k C_p)_w} \quad , \text{ where } T_{HN} = 324^{\circ}C \tag{12}$$

(6) Film Boiling Heat Transfer: The following modified Bromley correlation is adopted for the film boiling heat transfer[14];

$$q = C\left[\frac{k_g^3\gamma_g(\gamma_{\ell}-\gamma_g)h_{fg}'(1-\alpha)}{\mu_g\lambda_c(T_w-T_s)}\right]^{1/4}(T_w-T_s) \quad , \tag{13}$$

where $h_{fg}' = h_{fg}\left\{1+0.5\frac{G_g(T_w-T_s)}{h_{fg}}\right\}$, $\lambda_c = 2\pi\left(\frac{\sigma}{\gamma_{\ell}-\gamma_g}\right)^{1/2}$

and $C = 0.62$.

Table 1 summarizes the constitution of heat transfer package developed for the core thermal-hydraulic design and safety analysis of the new JRR-3.

IV CONCLUDING REMARKS

A heat transfer package was developed for the core thermal-hydraulic design and safety analysis of the new JRR-3. With the heat transfer package thus developed, the core thermal-hydraulic design has successfully been carried out.[17]

[Nomenclature]
A: Flow area, A_H: Heated area, C: Constant, C_p: Specific heat D_e: Equivalent hydraulic diameter, G: Mass flow rate, G^*: Dimentionless mass flow rate = $G/\sqrt{\lambda\gamma_g(\gamma_{\ell}-\gamma_g)g}$, g: Acceleration of gravity, h_{fg}: Latent heat of evaporation, Δh_i: Inlet subcooled enthalpy, k: Thermal conductivity, Nu: Nusselt number, P; Pressure, P_r: Prandtl number, q: Heat flux, q^*: Dimensionless heat flux = $q/h_{fg}\sqrt{\lambda\gamma_g(\gamma_{\ell}-\gamma_g)g}$, R_e: Reynolds number, T: Temperature, ΔT_s: Superheat, x: Quality, W: Width of channel, α: Void fraction, β: Volumetric expansion factor, γ: Specific weight, ρ: Density, ν: Kinematic viscosity, μ: Dynamic viscosity, λ: Critical wave length for DNB heat flux = $[\sigma/(\gamma_{\ell}-\gamma_g)]^{1/2}$, λ_c: Critical wave length for film boiling = $2\pi[\sigma/(\gamma_{\ell}-\gamma_g)]^{1/2}$, σ: Surface tension
[Subscript]
b: bulk, DNB: departure from nucleate boiling, f: film, g: steam, HN: homogeneous nucleation, ℓ: water, MSFB: minimum stable film boiling, ONB: onset of nucleate boiing, S: saturated, W: wall

References

(1) Bergles, A.E., et al.: Trans. ASME Ser. C, 86-3, 365 (1964).
(2) Dittus, F.W., et al.: Univ. Calif. Pubs. Eng., 2. 443 (1930).
(3) Clark, J.A., et al.: Trans. ASME, 76-2, 553 (1954).
(4) Hada, M.: Technical Memoranda, ISNSE, ANL, Oct. (1958).
(5) Sato, T., et al.: Trans. JSME, 29(204), 1367(1963), (in Japanese).
(6) Sieder, E.N., et al.: Ind. Eng. Chem., 28(12), 1429 (1933).
(7) Colburn, A.P.: AICHE J. 29, 174 (1933).
(8) Hwang, C-L., et al.: Appl. Sci. Res., Section A, vol. 13, 401 (1964).
(9) Mishima, K., et al.: Int. Mtg. on RERTR, Tokai, Japan, Oct. (1983).
(10) Mishima, K.: Boiling burnout at low flow rate and low pressure conditions, Dissertation Thesis, Kyoto Univ.
(11) Sudo, Y., et al.: J. Nucl. Sci. Technol., 22(3), 202 (1985).
(12) Collier, J.G.: "Convective Boiling and Condensation", McGraw Hill (1972), New York.
(13) Chen, J.C.: ASME paper NO. 63-HT-34, (1963).
(14) Sudo, Y., et al.: JAERI-M 84-066 (in Japanese).
(15) Bjonard, T.A., et al.: Symposium on Thermal and Hydraulic Aspects of Nuclear Reactor Safety, vol. 1, light water reactors, pp. 17-14, ASME., New York (1977).
(16) Henry, R.E.: AIChE Symposium Series, 138, vol. 70, pp. 81-90 (1974).
(17) Sudo, Y., et al.: J. Nucl. Sci. Technol., 22(7), 551 (1985).

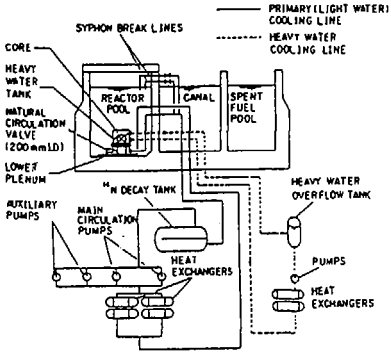

Fig. 1 Schematic diagram of the upgraded JRR-3 for core cooling

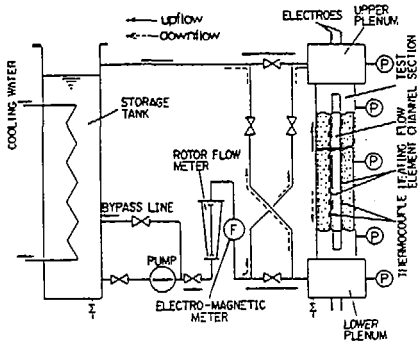

Fig. 2 Schematic diagram of experimental rig used for development of heat transfer package

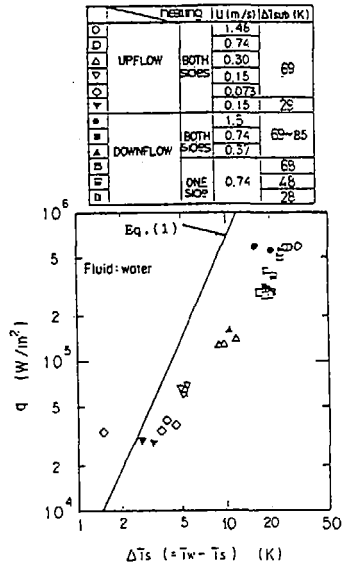

Fig. 3 Heat flux vs superheat at the ONB in downflow and upflow

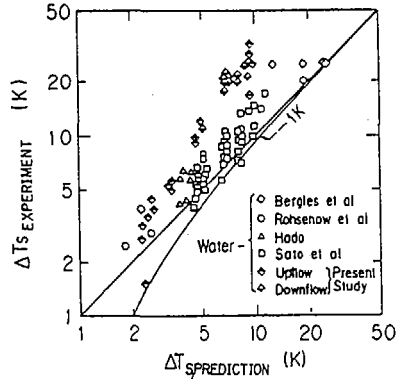

Fig. 4 Comparison between the measured and predicted superheats at the ONB with given heat flux

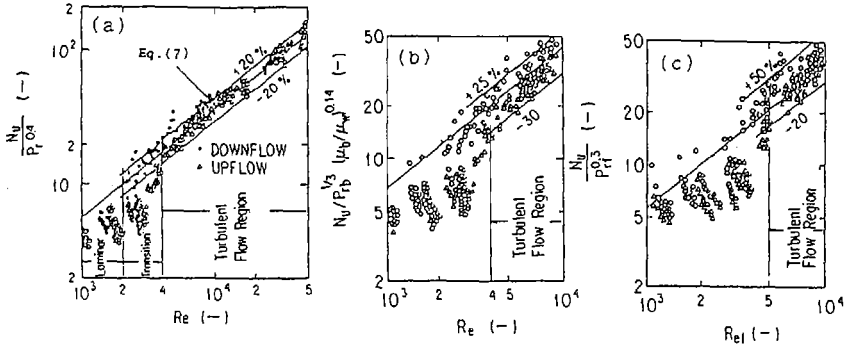

Fig. 5 Comparison of the experimental results with the existing correlations, (a) Dittus-Boelter's, (b) Sieder-Tate's and (c) Colburn's for turbulent flow on single-phase forced-convection heat transfer characteristics (Re ≳ 1000)

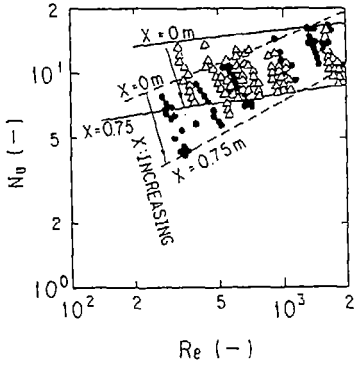

Fig. 6 Comparison of Nu vs Re between upflow and downflow fow Re less than 2000.

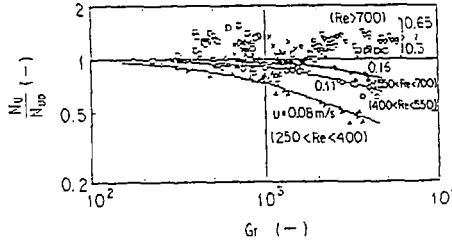

Fig. 7 Effects of Grashof Number on Nusselt Number in single-phase forced-convection laminar, downward flow

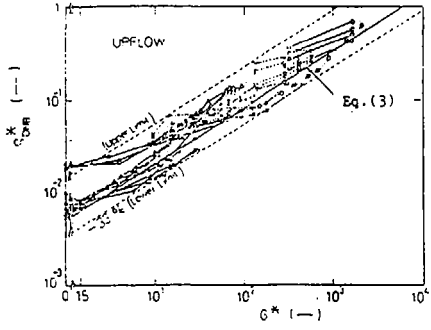

Fig. 8 Experimental results of DNB heat flux for upflow

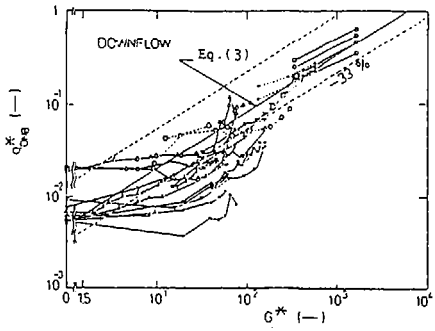

Fig. 9 Experimental results of DNB heat flux for downflow

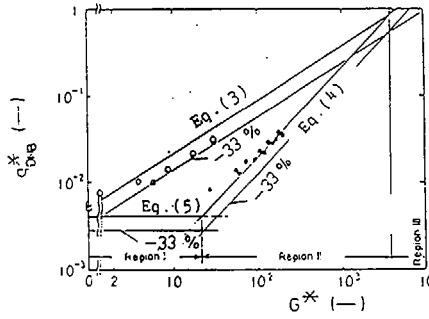

Fig. 10 Illustration of the proposed scheme of DNB heat flux correlations for upflow and downflow

Table 1 Constitution of the heat transfer package proposed for the design and analysis of the new JRR-3

Heat transfer mode		Downflow	Upflow
Single-phase flow	Laminar	Eq.(6)	Eq.(8)
	Transition	Interpolation	
	Turbulent	Eq.(7) (Dittus-Boelter)	
ONB temperature		Eq.(1) (Bergles-Rohsenow)	
Nucleate boiling	Subcooled	Eq.(10) (modified Chen)	
	Saturated	Eq.(10) (Chen)	
DNB heat flux		Min[Eq.(3), Max[Eq.(4), Eq.(5)]]	Max[Eq.(3), Eq.(5)]
Post-DNB Heat Transfer	Transition boiling	Eq.(11) (Bjornard-Griffith)	
	Minimum SPB temp.	Eq.(12) (Henry)	
	Film boiling	Eq.(13) (modified Bromley)	
	Steam single phase flow	The same as Liquid single phase flow	